FuelCell2008-65168

COMPARISON OF FEEDING GAS STRATEGIES (CO- AND COUNTER-FLOW) IN A PEM FUEL CELL THROUGH A PSEUDO 2D DIPHASIC WATER MODEL

Sylvain Chupin

LEMTA, CNRS / Nancy-université, Nancy, France

Institut de Recherche sur l'Hydrogène, UQTR, Trois-Rivières (QC), Canada

Julien Ramousse   Kodjo Agbossou   Yves Dubé

Institut de Recherche sur l'Hydrogène, UQTR, Trois-Rivières (QC), Canada

Sophie Didierjean   Gael Maranzanna

LEMTA, CNRS / Nancy-université, Nancy, France

ABSTRACT

The purpose of this study is to establish a simple model representing diphasic water flows in a single cell PEM fuel cell in order to improve fuel cell control. The pseudo-2D model describes the water transfers from one electrode to the other, all along the feeding gas channels. Both vapor and liquid water are considered. The location of first appearance of liquid water can be noticed. The influence of the feeding gas strategies (co- and counter-flow) on the water distribution in the cell are investigated. As a consequence, with the counter-flow feeding gas strategy, water is better distributed in the whole cell, but flooding of the electrode may occur. With a co-flow feeding gas strategy flooding risks are lower, but water distribution in the cell is less homogeneous and could result in a early deterioration of the membrane by drying.

NOMENCLATURE

D diffusive coefficient, $m^2.s^{-1}$
e thickness, m
EW membrane equivalent weight, $g.mol^{-1}$
F Faraday's constant, $C.mol^{-1}$
RH relative humidity, -
I current, A
K permeability, m^2

N molar flow, $mol.s^{-1}$
S saturation, -
SR gas stoichiometric ratio, -
T temperature, K
Greek letters
ε porosity, -
ρ_{dry} volumetric mass, $kg.m^{-3}$
λ membrane water content, -
Subscripts
AC anodic channel
AE anodic electrode
CC cathodic channel
CE cathodic electrode
α anodic liquid GDL fraction
γ cathodic liquid GDL fraction

INTRODUCTION

In Proton Exchange Membrane Fuel Cell (PEMFC) channels are made in bipolar plates to feed the reactant gases to the active areas and remove the electro-chemically produced water. Thus the water distribution in the cell highly depends on the gas feeding strategy in the channels [1],[2]. The hydration level of the cell, especialy the hydration of the membrane, is one of the key parameters for electrical efficiency [3],[4],[5], [6],[7]. The electrical resistance of the polymer membrane

1   Copyright © 2008 by ASME

directly depends on its water content [8]. The more there is water, the less the electrical membrane resistance is. However, too much liquid water could hinder reactive gases access to reaction sites (flooding) [9]. By reducing the reactions active area, the electrical efficiency of the cell decreases. An accurate description of the water distribution in the whole cell is needed to do a reliable prediction of the fuel cell performances. Moreover, the purpose of this model is to be added into a control device for fuel cells. The model must quickly compute the water distribution anywhere in the fuel cell for any operating conditions. Because of their high time of calculation, CFD (Computational Fluid Dynamics) codes are not appropriate to be used to control fuel cells [10],[11],[12]. The simulation have to be run in real time to develop a control tool. Only prevailing physical phenomena are modeled: only water (vapor and liquid) transfers are modeled and the currrent density is assumed homogeneous over all the cell. To illustrate this simplicity an electrical anology is used to represent water transfers in the cell. Our model is developed to find out how the water is distributed in the cell and how feeding gas strategies (co- and counter-flow) affect the water distribution. Whereas publications only show co-flow gas feeding models [13],[14].

WATER FLOW ACROSS THE CELL THICKNESS

The proton exchange membrane is sandwiched between the two electrodes to form the membrane-electrode assembly. On each side of this assembly, gas diffusion layers (GDL) allows the diffusion of reactant gases to the electrodes where the electro-chemical reactions occur. Reactant gases are fed to each GDL by the feeding channels made in the bipolar plates. In this paper, electrodes are so thin that they are not considered as an obstacle of water transport. Thus electrodes are assimilated to interfaces between GDLs and the membrane.

Mass flows in the fuel cell are complex because many components are present (water, oxygen, hydrogen) and water can be in different phases (vapor or liquid). The model presented here is a good compromise between physic complexity of transfers and simple calculation methods is presented. In this way, only the water transfer is studied in the cell thickness. The transport of the air and hydrogen from the channels to the electrodes is not modeled. A preliminary comparison with a multi-component Stefan-Maxwell diffusion model shows that reactant gas diffusion have an insignificant impact on water transport in the GDLs in standard conditions of simulation [15]. However, reactant gases consumptions are taken into account all along the feeding channels. Temperature and total pressure are assumed uniform in the whole cell.

Transfer through the polymer membrane

Water in the polymer membrane is liquid (adsorbed [16]). The polymer membrane is impervious to all other fluid. The Fick law gives the water flow as a function of water concentrations :

$$N_m^D = -D_m \frac{d C_W}{d z} \quad , \qquad (1)$$

D_m is the effective diffusion coefficient of water through the membrane. By definition, the water content (λ) of the membrane is linked to the water concentration in the membrane:

$$\lambda = \frac{EW}{\rho_{dry}} C_w \quad , \qquad (2)$$

EW is the membrane equivalent weight, and ρ_{dry} is the volumetric mass of dry membrane. Then, by writing concentrations as water contents on the edges of the membrane λ_{AE} et λ_{CE} , the diffusive water flow is:

$$N_m{}^D = D_m \frac{\rho_{dry}}{EW} \frac{\lambda_{AE} - \lambda_{CE}}{e_m} \quad . \qquad (3)$$

This flow is counted positively from the anodic electrode (AE) to the cathodic electrode (CE). Water contents λ_{AE} et λ_{AC} depend of the hydration state of the gases at the GDL/membrane interfaces. When water is only vapor, sorption curves links gas relative humidities (RH) to membrane water contents [17], [5]. Here, sorption curves are linearized :

$$\lambda_{AE} - \lambda_{CE} = k (RH_{AE} - RH_{CE}) \quad . \qquad (4)$$

If the membrane is immersed in liquid water, its water content λ_{liq} reaches a higher level than in a saturated gas $\lambda_{vap-sat}$: it's the Schroeder paradox [18].

Supposing that liquid water is in equilibrium with water saturated vapor, the resulting water content is written:

$$\lambda = (1-S)\lambda_{vap-sat} + S\lambda_{liq} \quad , \qquad (5)$$

where the saturation S is defined by the volumetric fraction occupied by liquid water over the total pore volume: $S = V_{liquid} / V_{pore}$.

If there is liquid water on each electrode, considering $\lambda_{liq} - \lambda_{vap-sat} \approx k$, leads to:

$$\lambda_{AE} - \lambda_{CE} = k (S_{AE} - S_{CE}) \quad . \qquad (6)$$

In each case (same water phases on both sides or not), the diffusive water flow thought the membrane is written:

$$N_m^D = \frac{X_{AE} - X_{CE}}{R_m} \quad , \qquad (7)$$

with $R_m = \frac{e_m EW}{D_m \rho_{dry} k}$ the mass transfer resistance and $X = RH$ for vapor water or $X = S$ for liquid water.

Protons have to cross the membrane from the anode to the cathode. Because protons are hydrated to move, an electro-osmotic water flow co-exist with the diffusive flow in the membrane. For a given current density I , this electro-osmotic flow is assumed constant. It is always oriented from the anode to the cathode and equal to :

$$N_m^{EO} = \xi \frac{I}{F} \quad . \qquad (8)$$

ξ is the number of water molecules transported by each moving proton. Here, it is chosen constant and equal to one [19].

Transfer through the GDL

Through GDLs, two models are developed to describe water transport: a first one if water is in vapor phase on each side of the GDL, another one if there is liquid water on these two sides. If there is liquid water on one side and vapor only at the other, a third model is developed as a combination of the two firsts.

Vapor phase transport

In the situation in which water is in vapor phase in all the GDL, the convective transport of vapor by the reactant gases crossing the GDLs is neglected. Then, water transport is purely diffusive so that Fick's law governed it.

$$N_{GDLvap} = -D_{GDL} \frac{d\,C_W}{d\,z} \qquad (9)$$

D_{GDL} is the effective diffusion coefficient of vapor water through the GDL. This coefficient is estimated from the GDL porosity ε and the diffusive coefficient of water into the gas (air or hydrogen) by the equation [20] :

$$D_{GDL} = \varepsilon^{1,5} D_{vapor \to gas} \qquad (10)$$

Introducing the relative humidity:

$$RH = \frac{P_{H_2O}}{P_{SAT}(T)} \qquad (11)$$

with $P_{SAT}(T)$ the saturation vapor pressure at the considered T temperature and P_{H_2O} the water pressure, the water concentration in the GDL can be written:

$$C_W = \frac{RH}{RT} P_{SAT}(T) \qquad (12)$$

with R the perfect gases constant.

Using equation (12) in the Fick's law (9) leads to express the vapor water flow through the GDLs as:

$$N_{GDLvap} = \frac{\Delta RH}{R_{GDL}} \qquad (13)$$

$R_{GDL} = \frac{e_{GDL} RT}{P_{SAT} D_{GDL}}$ and ΔRH is the relative humidity difference between each side of the GDL (channel and electrode).

Liquid phase transfers

If water is in liquid phase on both side of the GDL, Darcy's equation is used to described the water transport through the porous media:

$$v_w = -\frac{K K_r}{\mu_w} \frac{dP_{liq}}{dz} \qquad (14)$$

where v_w is the water flow velocity, K the permeability of the media, K_r its relative permeability, μ_w is the water dynamic viscosity and P_{liq} is the pressure of the liquid.

The liquid water flow is deduced from the water velocity:

$$N_{GDLliq} = \frac{\rho_w}{M_w} A v_w \qquad (15)$$

with ρ_w the water volumetric density, M_w its molar mass and A the area of the cell.

According to the capillary pressure definition: $P_{liq} = P_{cap} + P_{gas}$, with constant total gas pressure (P_{gas}), it can be written:

$$\frac{dP_{liq}}{dz} = \frac{dP_{cap}}{dz} \qquad (16)$$

Introducing saturations and combining equations 14, 16 and 15 lead to write the liquid water flow in the GDL [21]:

$$N_{GDLliq} = -\frac{\rho_w}{M_w} A \frac{K K_r}{\mu_w} \frac{dP_{cap}}{dS} \frac{dS}{dz} \qquad (17)$$

The capillary pressure model given by Brooks et Corey [22] links the capillary pressure to the saturation:

$$P_{cap} = \frac{p_d}{\sqrt[\lambda_B]{S}} \qquad (18)$$

P_d is the displacement pressure and λ_B is a pore distribution index. These numbers are given in the literature [23]. Burdine [24] gave a relative permeability model linking saturations and λ_B :

$$K_r = S^{\frac{2+3 \cdot \lambda_B}{\lambda_B}} \qquad (19)$$

Using equations (18) and (19) with the flow equation (17) leads to write the liquid water flow in the porous media as follow:

$$N_{GDLliq} = \frac{A_B}{e_{GDL}} \Delta S^{a_B} \qquad (20)$$

with $A_B = \frac{\rho_w}{M_w} A \varepsilon \frac{K}{\mu_w} P_d \left(\frac{1}{1+3\lambda_B}\right)$ and $a_B = \frac{1+3\lambda_B}{\lambda_B}$;
ΔS^{a_B} represents the gradient of saturations powered by a_B between GDL extremities.

Partially saturated GDL

In the case that water is liquid at only one side of the GDL (water is vapor at the other side), the GDL is split into two zones: a first one in which the transfer is in vapor phase and a second one where the transport follows liquid water equations. γ represents the cathodic GDL fraction in which the water flow is liquid, it determines the interface between liquid and vapor zones. At this interface $RH_y = 1$ and $S_y = 0$. In the same way, in the anodic GDL, this interface is noted α. Water can be liquid, independently in the channel or at the electrode. For instance, if the relative humidity is inferior to one in the cathodic channel and liquid water is present at the cathodic electrode (Figure 1), the water flow through the GDL $N_{GDL_{diph}}$ and the liquid fraction of GDL γ are solutions of the combination of liquid and vapor equations:

$$N_{GDL_{diph}} = \frac{A_B}{e_{GDL}\gamma} S_{CE}^{\alpha_B} \qquad N_{GDL_{diph}} = \frac{1-RH_{CC}}{R_{GDL}(1-\gamma)} \qquad (21)$$

3

Copyright © 2008 by ASME
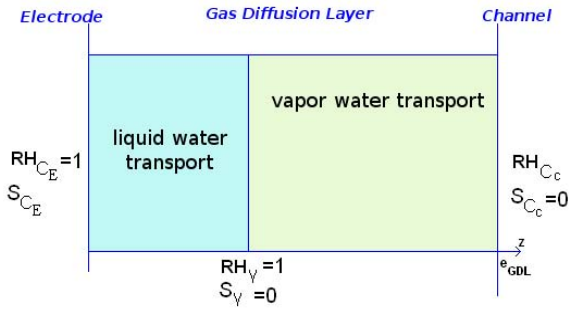
Figure 1: Partially saturated cathodic gas diffusion layer (GDL) scheme

Electrical analogy

In the cell thickness, the water transport from a channel to the other is compute in a 1D element representing the fuel cell assembly. The modeling in 1D elements is based on an electrical analogy. When in electricity we use currents here we use water flows. Likewise, electrical potentials are replaced by relative humidities of gases (or saturations). The scheme can be represented as on Figure 2.
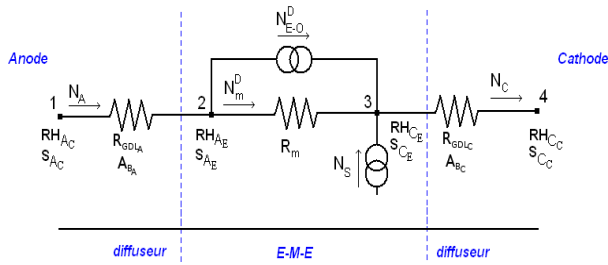
Figure 2: Electrical analogy scheme

Potentials are studied at the four key interfaces of the fuel cell only: (1) anodic channel/anodic GDL, (2) anodic GDL/membrane (anodic electrode), (3) membrane/cathodic GDL (cathodic electrode), (4) cathodic GDL/cathodic channel. The electro-chemical water production at the cathodic electrode is represented by a punctual water source at the interface between the membrane and the cathodic GDL. The water flow in the membrane is a combination of a diffusive flow and an constant electro-osmotic flow.

Thus water flows thought the two GDLs and the membrane have to be calculated as a function of the hydration conditions of the gases in the channels (potentials). If water is only vapor at the interface points, potentials used are relative humidities. In this case the water transport model is linearized and the electrical analogy is perfectly justified. When liquid water appears in GDLs or channels ($RH=1$), saturations are used as potentials. In that case, even if equations are not linear, the electric scheme (with linear resistances) is kept for more clarity.

Resolving the 1D water transport in the cell thickness leads to solve a problem of 5 equations with 5 unknowns. If water is in the same phase on each side of the GDLs, the 5 equations are : 1 in the membrane (7), 1 in each GDL (13 or 20) and 1 at

each electrodes (node 2 and node 3 of Figure 2). The 5 unknowns are : three water flows (in the anodic and cathodic GDLs and in the membrane) and two "potentials" (at the electrodes). If water phases are different on each side of the GDL, one more equation (21) and a additional unknown (α or γ) are needed in each GDL. At last, up to 7 equations with 7 unknowns have to be solved.

On each four characteristic points, water can be in liquid phase or in vapor phase. Hence, 16 different 1D transfer cases would exist. But 4 of these cases are not physically acceptable. Thus, 12 credible physical cases could occur for the 1D water transport in the cell thickness.

Studying the limits ($RH=1$ or $S=0$ at one of the 4 characteristic points) between these 12 cases leads to calculate the liquid water appearance limits at the 4 points of the cell thickness. These limits are analytically calculated and drawn.

PSEUDO 2D WATER TRANSFER IN THE CELL

From the gas inlet to the outlet the cell is discretized in N elements. In each elements, the transport through the GDLs and the membrane is computed with the previously presented 1D models. 1D modelings lead to calculate all flows (through GDL and membrane) and potentials (at the electrodes) through a discrete element. The second dimension of the modeling comes from mass balances done in the channels of each discrete elements (Figure 3). Mass balances allow to compute the advance of water and reactant gas concentrations along the feeding channels.
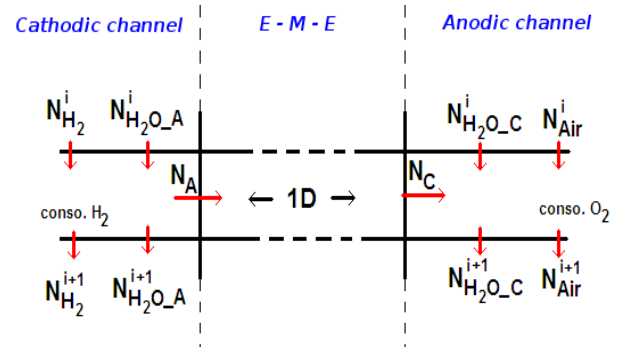
Figure 3: Pseudo-2D mass balances scheme

Steady state is considered here. Mass balances for water and reactant gases are written:

Anodic channel :
$$N_{H_2O\_A}^{i+1} = N_{H_2O\_A}^{i} - N_A^{i}$$
$$N_{H2}^{i+1} = N_{H2}^{i} - \frac{1}{N}\frac{I}{2F}$$
(22)

And

Cathodic channel :
$$N_{H_2O\_C}^{i+1} = N_{H_2O\_C}^{i} + N_C^{i}$$
$$N_{Air}^{i+1} = N_{Air}^{i} - \frac{1}{N}\frac{1}{0,21}\frac{I}{4F}$$
(23)

4

Copyright © 2008 by ASME

Reactant gases transport in the cell thickness are not considered, but their consumptions are subtracted to flows in the channels. Knowing water flows and reactant gases flows in the next element allows to compute the channel potentials (RH or S) in the next discrete element.

As the current is assumed uniform in all the cell, each discrete element produce the same current. The uniformity of the current distribution is the main assumption in this work. However, according to the high electrical conductivity of the cell components (particularly carbon made bipolar plates), it rather be the electric potential that should be uniform. Thus, the assumption of an homogeneous current distribution has a strong impact on the results. This particular point will be uppermost dealt with in the future.

Different feeding gas strategies can be investigated. Supposing that bipolar plates are the same at the cathode and at the anode, reactant gases can be distribute in different way on each side of the cell. If, in the feeding channels, hydrogen and air flows are parallels and going in the same direction, the strategy is called co-flow (Figure 4). If the feeding gases flows are parallels but are going in opposite ways, the strategy is called counter-flow.(Figure 4). Cross-flow (perpendicular air and hydrogen channel flows) strategies also exist, but they are not yet modeled.
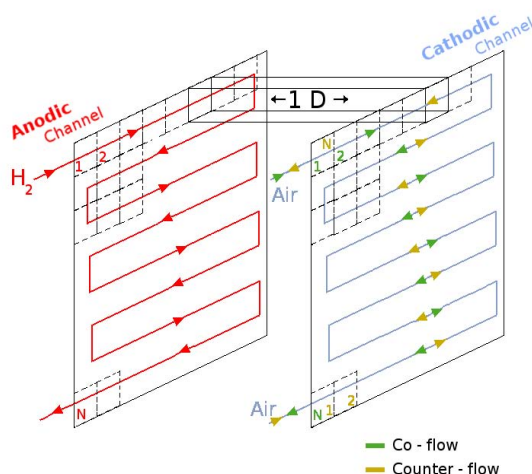
Figure 4: co- or counter-flow reactant gas strategies

The counter-flow modeling differs on two points with the co-flow one. First, the air inlet corresponds to the hydrogen outlet and vice-versa. Secondly, mass balances in the cathodic channel are inversed. Figure 3 represents mass balances for a co-flow strategy (air and hydrogen flow in the same direction). For a counter-flow strategy, flow in the cathodic channel are in the opposite way, so that mass balances equations have to be adapted. Then, influences of these two feeding gas strategies on the water distribution in the cell are analyzed.

SIMULATION RESULTS

The co-flow and the counter-flow feeding gas strategies are simulated with the model presented. First, simulation results of

each strategies are investigated, then these results are compared to find out which strategy leads to the better water distribution.

Co- and counter-flow results

For each feeding gas strategies, simulation parameters are the same:

$I = 0.5\ A.cm^{-2}$	$N = 1000\ (\text{discrete elements})$
$P = 1\ atm$	$P_d = 0.102\ 10^5\ Pa$
$T = 60\ ^\circ C$	$\lambda_B = 1.59$
$SR_{H_2} = 2$	$\varepsilon = 0.8$
$SR_{Air} = 2$	$EW = 1100\ g.mol^{-1}$
$e_{membrane} = 37\ \mu m$	$\rho_{dry} = 2020\ 10^3\ g.m^{-3}$
$e_{GDL} = 280\ \mu m$	$K = 2.55\ 10^{-12}\ m^2$
$A = 78\ cm^2$	

Table 1: Standard simulation parameters

Co-flow feeding gas strategy.

Feeding gases (hydrogen and air) are introduced in the fuel cell inlet with given relative humidities (RH_{CC}^{IN} and RH_{AC}^{IN}). The Figure 5 allows to follow the relative progression of potentials (relatives humidities and saturations) in one channel as a function of the other. Two simulations results are shown: a first one if air is dry at the inlet and the hydrogen is humidified (50%), a second one with the opposite inlet gases humidification conditions (dry hydrogen and humidified air).
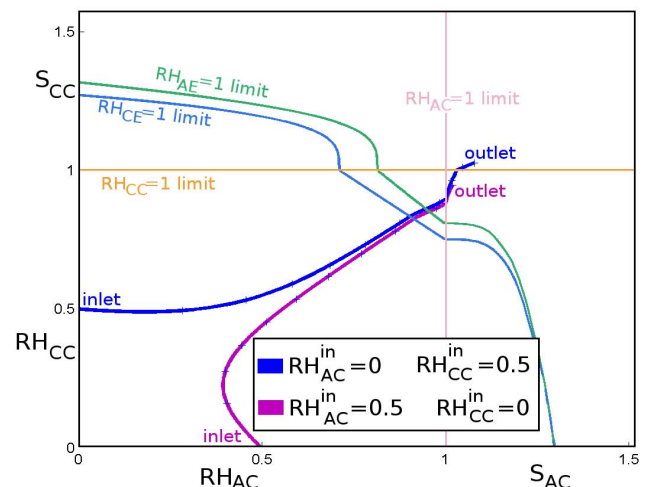
Figure 5: Map of potentials in the channels, co-flow

On Figure 5 liquid water appearance limits in the cell thickness are also drawn. Knowing potentials in the two feeding channels leads to know in which phase water is at the electrodes. Then, the crossing of theses limits correspond to the appearance of liquid water in one of the 4 characteristic point of the cell thickness.

Thus, following the blue curve on Figure 5 ($RH_{CC}^{IN} = 0$ and $RH_{AC}^{IN} = 0.5$) leads to find out how liquid water appears in the fuel cell. At the beginning of the flow all fluids are in vapor phase. Then, liquid water appears at the cathodic electrode ($HR_{CE} = 1$ limit). Next, liquid water appears at the anodic electrode ($HR_{AE} = 1$ limit). After that, liquid water appears in

5

Copyright © 2008 by ASME

the anodic channel ($HR_{AC}=1$ limit). And finally, there is liquid water in the cathodic channel ($HR_{CC}=1$ limit).

For these two simulations, near the flow inlet, the relative humidity in the humidified channel decreases. So if $RH_{CC}^{IN}=0$ and $RH_{AC}^{IN}=0.5$ (purple curve on Figure 5), we observe that the relative humidity in the anodic channel decrease just after the inlet while the relative humidity in the cathodic channel highly increase. Water introduced by the hydrogen tends to humidify dry air fed at the cathode.

This diffusive phenomena results in an equilibrium between anodic and cathodic compartment of the cell. After a certain length of the channel, no matter if the water was introduced at the anode (with the hydrogen) or at the cathode (with the air) sides, the water distribution is roughly the same.

But, by comparing the two simulations presented on Figure 5, one can notice that if air is humidified at the inlet (blue curve) there is liquid water at the two channels outlet. Whereas if the hydrogen is humidified at the inlet (purple curve), liquid water is only present at the anodic channel outlet. The two simulations do not show the same outlet states because water quantities introduced in the cell were not the same, only relative humidities were.

Other simulations have been done introducing the exact same water quantity (instead of relative humidities) once in the hydrogen, once in the air (Table 2). The humidifying water introduced in the feeding gases correspond to 50% of the electro-chemically produced water. Hence, water going out from the cell is equal to 150% of the produced water (water produced + humidification water).

Inlet [anodic water, cathodic water] (% of produced water)	Outlet [anodic water, cathodic water] (% of produced water)
[0 , 50]	[34.4 , 115.6]
[50 , 0]	[34.7 , 115.3]
[25 , 25]	[34.5 , 115.5]

Table 2: Outlet water distribution in function of inlet humidifying conditions, co-flow

Thus, regardless of how gases are humidified, the water distributions in the anodic and cathodic outlets are the same. Because produced water depends on the current density and is produced at the cathodic electrode, this outlet water distribution is correlated with the current density of the cell.

The same simulations have been done for a counter-flow feeding gas strategy.

Counter-flow feeding gas strategy

The same representation is used for counter-flow feeding gas strategy. The Figure 6 represents the progression of potentials in the cathodic channel as a function of the potentials in the anodic one.

As in the co-flow strategy, the results given by the

simulation in which inlet hydrogen is dry and air is humidified (blue curve on Figure 6) are analyzed in detail to determined the distribution of liquid water in the cell.
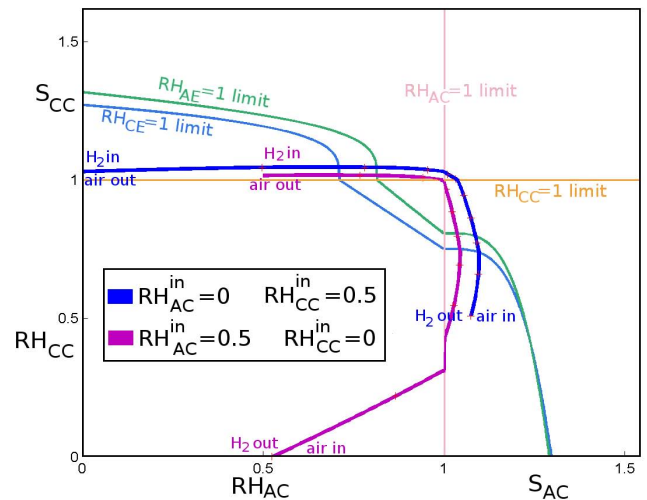
Figure 6: Map of potentials in the channels, counter-flow

The channels are in opposite ways so we follow the hydrogen way to analyze the water distribution. The inlet of the hydrogen channel correspond to the air channel outlet. That's why there is liquid water in the cathodic channel while hydrogen is introduced in the cell. Then liquid water appears at the cathodic electrode. After that there is liquid water at the two electrodes and in the cathodic channel. Thus liquid water appears in the anodic channel: water is liquid in the whole cell thickness. Close to the air inlet (hydrogen outlet), air is dryer so potentials in the cathodic compartment decrease. First, liquid water disappears in the cathodic channel, then at the anodic electrode and finally at the cathodic electrode. At the hydrogen outlet water is liquid in the anodic channel whereas air is introduced with the given relative humidity.

With the counter-flow feeding gas strategy, humidifying air or hydrogen do not lead to the same water distribution between cathodic and anodic channels at the outlets (Table 3).

Inlet [anodic water, cathodic water] (% of produced water)	Outlet [anodic water, cathodic water] (% of produced water)
[0 , 50]	[35.3 , 114.7]
[50 , 0]	[17.2 , 132.8]
[25 , 25]	[24.2 , 125.8]

Table 3: Outlet water distribution in function of inlet humidifying conditions, counter-flow

An interesting result is that humidifying air (at the cathode) gives more water at the anodic channel outlet. This is normal because inlet humidified air humidify the hydrogen exiting of the cell.

By comparing the two simulations presented on Figure 6, one can notice that when air is humidified at the inlet (blue

6

Copyright © 2008 by ASME

curve) there is liquid water at the two channels outlet. Whereas when hydrogen is humidified at the inlet (purple curve), liquid water is only present at the cathodic channel outlet. Once again, the vapor at the hydrogen inlet humidify the exiting air and, the non humidified inlet air dry the exiting hydrogen.

Results of the two feeding gas strategies are more precisely compare in the next part.

Co- and counter-flow comparison

Feeding gas strategies drastically change the water distribution in the cell. To compare co- and counter-flow water distributions, Figure 7 represents the progression of relative humidities and saturations along the cell for the two feeding strategies. This figure is another representation of the blue curves of the Figure 5 and Figure 6 (air is introduced with a 50% relative humidity ($RH_{CC}^{IN} = 0,5$), and inlet hydrogen is dry ($RH_{AC}^{IN} = 0$)). Simulations have been done with Table 1 parameters.

As mentioned, performances of fuel cells are directly linked to water distribution. On the one hand, the better the membrane is hydrated the better protons can pass thought the membrane. Moreover, membrane properties can be spoiled if it dries out. Fuel cell performances would be better and for a longer time if the membrane is not too dry. On the other hand, if the amount of liquid water is too large at the electrodes, electro-chemical reaction sites can be flooded. Hence, the best hydration conditions are nearly reached while relative humidities are one and saturations are null at the two electrodes.
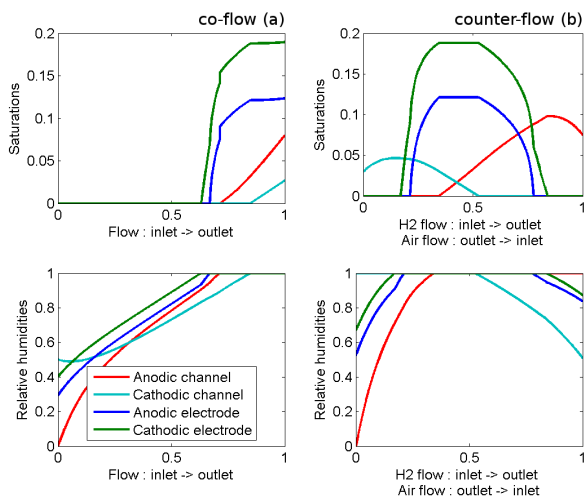
Figure 7: Relative humidities and saturations along the cell, co- and counter-flow comparison

A detailed exploitation of the results presented on Figure 7(a) gives the complete distribution of water in the cell for a co-flow feeding strategy. In 63% of the cell, water is only vapor. In 4% there is liquid water only at the cathodic electrode. In 5% liquid water is present on the two electrodes. Then in 13% of the cell there is liquid water at the two electrodes and in the anodic channel. Finally, in the last 15% of the cell there is liquid water in all the cell thickness.

Moreover the same analysis is done for Figure 7(b), to describe the water distribution in a counter flow feeding strategy. In term of cell surface, in 35% of the cell water is liquid in the cathodic channel. For 67% of the flow there is liquid water at the cathodic electrode. Among it, 56% of the flow also results in liquid water at the anodic electrode. And, in 65% of the cell water is liquid in the anodic channel.

Then, a main difference in the water distributions for the two feeding gas strategies is the relative humidities values in absence of liquid water. With the counter-flow strategy, in absence of liquid water, relative humidities are quite high. At the electrodes relatives humidities are always above 50%. On the other hand, the co-flow simulation shows quite low relative humidities close to the inlets. In the first 17% of the cell, relative humidities at the electrodes are below 50%. This bad humidification of the membrane could lead to a early deteriorations of the polymer membrane, and by this way a decrease of the fuel cell performances.

Figure 7 shows that with a co-flow strategy water high potential areas are concentrated close to the end of the flow while with the counter-flow distribution, water is spread likely in the whole cell. With the counter-flow strategy there is always liquid water in one of the 4 key points of the cell. This better distribution of water in all the cell is particularly good for membrane hydration. Water is liquid on each side of the membrane for 56% of the cell with the counter-flow feeding gas strategy whereas there is only 33% of the cell in which there is liquid water on both side of the membrane for the co-flow strategy. This better hydration of the protonic membrane would give better electrical performances with a counter-flow fed fuel cell.

However, the good hydration of the membrane with a counter-flow feeding strategy is attenuate by the fact that more liquid water is present. As saturations for the two simulations reach the same level (19%), flooding is equally important in the two feeding strategies, but it concerns a larger part of the cell in the counter-flow simulation (67% of the counter-flow strategy, 37% for the co-flow strategy). To conclude, the counter-flow strategy is more prone to flooding.

CONCLUSIONS

A model have been developed to study the water distribution in a PEM fuel cell. The water distribution was analyzed from the gas inlet to the outlet and through the cell thickness. The liquid water as the vapor water are taken into account in the model. Thereby liquid water appearance and transport were studied. This model allows also to simulate and compare two feeding gas strategies. A co-flow strategy, in which air and hydrogen flow in the same way, is compared with a counter-flow strategy in which air and hydrogen are flowing in opposite ways.

The counter-flow model gives a better distribution of water in the whole cell. The water is not concentrate next to the outlets but it is more homogeneously distributed everywhere. In consequence of this water distribution, feeding fuel cells with counter-flow strategy can prevent early deteriorations of the polymeric membrane by drying. Also, the membrane is

7

Copyright © 2008 by ASME

better humidified, so electrical performances of the cell might be better. However, more liquid water is noticed for this strategy. Thus, active area flooding could occur, that results in drastic electrical performances drops.

A set of experiments is planned to validate this model and its results. Moreover, to improve the accuracy of the model the assumption of a uniform current distribution will be changed into a uniform electric potential distribution model. Then, the evolution of current density along the cell channels would be observed. This will allow to directly estimate the impact of water distribution on cell performances. Comparing these results with a cross-flow feeding gas strategy could also be interesting.

REFERENCES

[1] : F.Chen, Y.Wen, H.Chu, W.Yan and C.Soon, 2004, "Convenient two-dimensional model for design of fuel channels for proton exchange membrane fuel cells", *J. power sources*, 128, 125-134.

[2] : J.S.Yi and T.V.Nguyen, 1998, "An Along-the-Channel Model for Proton Exchange Membrane Fuel Cells", *J. Electrochem. Soc.*, 145(4), 1149-1159.

[3] : D.M.Bernardi, 1990, "Water-Balance Calculations for Solid-Polymer-Electrolyte Fuel Cells", *J. Electrochem. Soc.*, 137(11), 3344-3350.

[4] : T.Okada, G.Xie and Y.Tanabe, 1996, "Theory of water management at the anode side of polymer electrolyte fuel cell membranes", *J. Electroanalytical Chemistry*, 413(1-2), 49-65.

[5] : T.E.Springer, T.A.Zawodzinski and S.Gottesfeld, 1991, "polymer electrolyte fuel cell model", *J. Electrochem. Soc.*, 1388, 2334-2342.

[6] : T.V.Nguyen and R.E.White, 1993, "A Water and Heat Management Model for Proton-Exchange-Membrane Fuel Cells", *J. Electrochem. Soc.*, 140(8), 2178-2186.

[7] : T.F.Fuller and J.Newman, 1993, "Water and Thermal Management in Solid-Polymer-Electrolyte Fuel Cells", *J. Electrochem. Soc.*, 140(5), 1218-1225.

[8] : T.Okada, G.Xie and M.Meeg, 1998, "Simulation for water management in membranes for polymer electrolyte fuel cells", *Electrochimica Acta*, 14-15(43), 2141-2155.

[9] : H.Li, Y.Tang, Z.Wang, Z.Shi, S.Wu, D.Song, J.Zhang, K.Fatih, J.Zhang, H.Wang, Z.Liu, R.Abouatallah and A.Mazza, 2007, "A review of water flooding issues in the proton exchange membrane fuel cell", *J. power sources*, 178, 103-117.

[10] : J.Jang, W.Yan and C.Shih, 2006, "Numerical study of reactant gas transport phenomena and cell performance of proton exchange membrane fuel cells", *J. power sources*, 156, 244-252.

[11] : Z.H.Wang, C.Y.Wang and K.S.Chen, 2001, "Two-phase flow and transport in the air cathode of proton exchange membranefuel cells", *J. power sources*, 94, 40-50.

[12] : S.Shimpalee, S.Greenway, D.Spuckler and J.W.Van Zee, 2004, "Predicting water and current distributions in a commercial-size PEMFC", *J. power sources*, 135, 79-87.

[13] : D.Singh, D.M.Lu and N.Djilali, 1999, "A two-dimensional analysis of mass transport in proton exchange membrane fuel cells", *Int. J. Eng. Science*, 37(4), 431-452.

[14] : W.He, J.S.Yi and T.V.Nguyen, 2000, "Two-phase flow model of the cathode of PEM fuel cells using interdigitated flow fields", *AIChE J.*, 46(10), 2053 - 2064.

[15] : J.Ramousse, 2005, "Transferts couplés masse-charges-chaleur dans une cellule de pile à combustible à membrane polymère", PhD thesis, LEMTA - INPL.

[16] : M.Laporta, M.Pegoraro and L.Zanderighi, 1999, "Perfluorosulfonated membrane(Nafion): FT-IR study of the state of water with increasing humidity", *Physical Chemistry Chemical Physics*, 1, 4619–4628.

[17] : J.T.Hinatsu, M.Mizuhata and H.Takenaka, 1994, "Water uptake of perfluorosulfonic acid membranes from liquid water and water vapor", *J. Electrochem. Soc*, 141(6), 1493-1498.

[18] : P.Schroeder, 1903, "Uber Erstarrungs–und Quellungserscheinungen von Gelatine", *Z. Phys. Chem.*, 45, 57.

[19] : T.A.Zawodzinski, J.Davey, J.Valero and S.Gottesfeld, 1995, "The water content dependance of electro-osmotic drag in proton conducting polymer electrolytes", *Electrochemical Acta*, 403, 297-302.

[20] : A.Souto, 1993, "Diffusion-dispersion en milieux poreux : étude numérique du tenseur de dispersion pour quelques arrangements périodiques bidimensionnels ordonnés et désordonnés", PhD thesis, LEMTA - INPL.

[21] : J.H.Nam and M.Kaviany, 2003, "Effective diffusivity and water-saturation distribution in single- and two-layer PEMFC diffusion medium", *Int. J. Heat and Mass Transfer*, 46, 4595-4611.

[22] : R.J.Brooks and A.T.Corey, 1964, "Hydraulic properties of porous media", *Hydrol. Pap.*, 3, .

[23] : J.T.Gostick, M.W.Fowler, M.A.Ioannidis, M.D.Pritzker, Y.M.Volfkovich and A.Sakars, 2006, "Capillary pressure and hydrophilic porosity in GDL for PEMFC", *J. of power sources*, 156, 375-387.

[24] : N.T.Burdine, 1953, "Relative permeability calculations from pore size distribution data", *Trans.of the Am. Inst. of Min. and Metal. eng.*, 198, 71-78.

Copyright © 2008 by ASME